Assessment of Constant Envelope OFDM as a Class of Random FM Radar Waveforms

Erik R. Biehl[1], Charles A. Mohr[1,2], Brandon Ravenscroft[1], Shannon D. Blunt[1]
[1] Radar Systems Lab (RSL), University of Kansas, Lawrence, KS
[2] Sensors Directorate, Air Force Research Laboratory (AFRL), Wright-Patterson AFB, OH

***Abstract*—Random FM radar waveforms designed to possess a desirable spectral shape (on average) have been experimentally demonstrated for an increasing number of applications. However, the benefits of these waveforms can be offset by the computational cost of performing real-time spectral-shaping optimization for each random initial waveform. Here the constant-envelope orthogonal frequency division multiplexing (CE-OFDM) framework from communications is examined as a means to generate random FM radar waveforms. This scheme is attractive from a radar perspective because it inherently provides useful spectrum shaping without the need for optimization, thereby realizing an effective form of random FM that can be produced in real-time on systems with modest computational resources, in addition to the obvious communication capability. Radar performance is assessed in simulation and using free-space experimental measurements.**

Keywords—waveform diversity, FM noise, pulse agility

I. INTRODUCTION

Random FM (or FM noise) waveforms can originally be traced back to a US Navy patent filed in 1956 by Whiteley and Adrian that was issued in 1980 [1]. Subsequent work on the subject was performed by Guosui, et al, in China during the 1990's [2], by Axelsson in the early 2000's in Sweden [3], and more recently by Pralon, et al, in Brazil [4]. A consistent theme through these efforts has been a focus on the use of white noise to drive the frequency modulation of the random signal.

In contrast, the notion of spectrally-shaped random FM (RFM) has in recent years been experimentally demonstrated using a variety of different approaches to perform the shaping and for a number of different applications (see [5] for an overview). The primary benefit of spectrum shaping is to realize good waveform autocorrelation properties (i.e. low range sidelobes while preserving the mainlobe) on a per-pulse basis (or per-segment if CW [6]).

However, performing this spectral shaping does incur some computational cost depending on how it is performed, bearing in mind that shaping of the spectral roll-off region is just as important as shaping the in-band region, and also that the FM structure must be maintained for each waveform to be amenable to high-power radar transmission. The approaches considered thus far include forms of alternating time/frequency projections [6-9], applications of gradient descent [10,11], and most recently an offline optimization approach to construct a framework that shapes a white noise process [12].

The latter of these, denoted as stochastic waveform generation (StoWGe), is the only one that does not require real-time optimization to produce new RFM waveforms. Of course, StoWGe does still require offline optimization to obtain the spectral shaping framework that is applied in real-time.

Here we consider another approach that, while not having quite the degree of design freedom of these other methods, has the interesting benefit of realizing a desirable spectral shape (on average) for RFM without the need for any spectral-shaping optimization whatsoever. This approach is based on the CE-OFDM communication signal structure [13-16] and builds upon subsequent work [17-22] that sought to apply this scheme to radar (or dual-function radar/communications). Specifically, [17-21] rely upon real-valued constellations of modulating symbols such as BPSK or a multi-level form like pulse amplitude modulation (PAM). The authors of [22] also generalize this framework to complex constellations such as quadrature amplitude modulation (QAM).

In some of these cases the selection of symbol values (i.e. code design) is considered as a means to realize a particular waveform with low range sidelobes. Alternatively, in [21] the remediation of pulse-to-pulse range sidelobe modulation (RSM) [23] is addressed by introducing a parameter to control the sidelobe variation similar to that proposed in [24] for continuous phase modulation (CPM) implementation.

Here we examine the utility of the CE-OFDM signal structure for RFM radar applications, where a goal is to maximize the diversity among the set of waveforms in the coherent processing interval (CPI) while maintaining roughly the same power spectrum content. To that end, the complex constellation framework from [22] is employed for different numbers of subcarriers and different symbol constellation densities to assess the efficacy of CE-OFDM for utility as an optimization-free class of RFM radar waveforms. The dual-function radar/communication (DFRC) attribute, a topic of much interest in its own right (e.g. [25-29]), is thus a natural occurrence of this waveform structure.

II. CE-OFDM SIGNAL STRUCTURE

Fourth generation (4G) and emerging 5G cellular communication systems employ OFDM because it makes efficient use of spectrum and is easy to demodulate and equalize. The baseband representation for one symbol interval T of an OFDM signal can be expressed as

$$u(t) = \sum_{n=1}^{N} \beta_n \exp(j2\pi f_n t) , \qquad (1)$$

This work was supported by the Office of Naval Research under Contract #N00014-20-C-1006 and by a subcontract with Matrix Research, Inc. for the Air Force Research Laboratory under Prime Contract #FA8650-14-D-1722. DISTRIBUTION STATEMENT A. Approved for Public Release.

978-1-7281-8942-0/20/$31.00 ©2020 IEEE

where β_n is the communication symbol (based on some constellation) for the nth subcarrier, which is the corresponding complex sinusoid with frequency f_n. To preserve orthogonality for communication purposes the subcarrier frequencies are separated by $1/T$. Because (1) is comprised of a weighted sum of complex sinusoids, the envelope of $u(t)$ is clearly not constant and high power efficiency on transmit (via amplifier saturation) is not possible.

Consequently, CE-OFDM [13-16] was proposed as an alternative communication implementation that does realize a constant envelope signal, though other trade-offs do arise. For application in the radar context we shall use the form from [22] that expresses CE-OFDM as

$$s(t) = \exp\left(j2\pi h \, \Re\left\{ \sum_{n=1}^{N} \beta_n \exp(j2\pi f_n t) \right\} \right) \text{ for } 0 \le t \le T, \quad (2)$$

in which $2\pi h$ is the modulation index, T is now the radar pulse width, and $\Re\{\cdot\}$ extracts the real part of the argument, which in this case is the complex OFDM signal from (1). It is easy to show that (2) can likewise be expressed as

$$s(t) = \exp\left(j2\pi h \sum_{n=1}^{N} \left|\beta_n\right| \cos(2\pi f_n t + \phi_n) \right) \quad (3)$$

where ϕ_n is the phase of symbol β_n. Thus this form is a generalization of those in [17-21], which involve a weighted sum of cosines, by allowing their phases to vary as well, consequently providing greater freedom for each individual waveform that is produced in this manner.

If we now compactly express the terms in (3) as

$$z_n = 2\pi h \left|\beta_n\right| \quad (4)$$

and

$$\theta_n(t) = 2\pi f_n t + \phi_n, \quad (5)$$

then (3) can also be written as

$$s(t) = \exp\left(j \sum_{n=1}^{N} z_n \cos\left(\theta_n(t)\right) \right), \quad (6)$$

which is equivalent to

$$s(t) = \prod_{n=1}^{N} \exp\left(j z_n \cos\left(\theta_n(t)\right) \right). \quad (7)$$

As previously leveraged for CE-OFDM [14] and more recently for the related multi-tone feedback FM (MT-FFM) waveform design approach by Hague and Kuklinksi [30], the Jacobi-Anger expansion [31] of each exponential term in (7) yields

$$\begin{aligned} s(t) &= \prod_{n=1}^{N} \sum_{m=-\infty}^{\infty} j^m J_m(z_n) \exp\left(jm\, \theta_n(t) \right) \\ &= \prod_{n=1}^{N} \sum_{m=-\infty}^{\infty} j^m J_m\left(2\pi h \left|\beta_n\right|\right) \exp\left(jm(2\pi f_n t + \phi_n) \right) \end{aligned}, \quad (8)$$

where $J_m(\bullet)$ is the mth Bessel function of the first kind and in the lower part of (8) we have resubstituted for (4) and (5).

Now collecting the constant terms in (8) together as

$$d_{n,m} = j^m J_m\left(2\pi h \left|\beta_n\right|\right) \exp\left(jm\phi_n \right) \quad (9)$$

we obtain the waveform representation

$$s(t) = \prod_{n=1}^{N} \sum_{m=-\infty}^{\infty} d_{n,m} \exp\left(j2\pi m f_n t \right) \text{rect}\left(\frac{t - T/2}{T} \right), \quad (10)$$

where inclusion of the rect(•) function explicitly indicates the pulsed time support on [0, T]. Thus each term in the repeated product of (10) is comprised of an infinite sum of complex sinusoids that are weighted by the Bessel function envelope and truncated to a temporal extent of T.

Consequently, the Fourier transform of each infinite sum in (10) is a like-weighted infinite set of sinc(•) functions in the frequency domain, centered at frequency offset $m f_n$. Moreover, since each repeated product becomes a repeated convolution in the frequency domain, the central limit theorem implies that the overall spectral content of $s(t)$ will tend toward a Gaussian shape (on average) as N and h gets large, to the degree possible for a rectangular pulse shape.

Note that while standard OFDM, and by extension CE-OFDM, would generally rely on the use of a cyclic prefix (CP) to avoid intersymbol interference (ISI) and to simplify equalization in the communication context, doing so for radar is expected to introduce a significant range sidelobe due to the inherent repetition involved. From a DFRC perspective, the pulsed structure does avoid the ISI issue if symbol interval is the same as the pulse width, though equalization is a bit more complicated. For instance, the latter can be achieved via a zero-forcing approach such as that employed for the tandem-hopped radar/communications (THoRaCs) experimental demonstration in [32].

III. INSTANTANEOUS FREQUENCY

In [15] the root-mean-squared (RMS) bandwidth (in Hz) for CE-OFDM is specified as

$$B = 2\pi h \left(N/T \right), \quad (11)$$

assuming the subcarriers are symmetric about the carrier frequency (0 at baseband) and as long as $2\pi h > 1$, in which case the expected power spectrum is Gaussian. Because CE-OFDM also represents a form of FM, it is likewise instructive to consider the instantaneous frequency. If we define the continuous, instantaneous phase from (3) as

$$\phi(t) = 2\pi h \sum_{n=1}^{N} \left|\beta_n\right| \cos(2\pi f_n t + \phi_n), \quad (12)$$

such that (3) becomes $s(t) = \exp(j\phi(t))$, then instantaneous frequency (in Hz) can be expressed as

$$f(t) = \frac{1}{2\pi} \frac{d\phi(t)}{dt}. \quad (13)$$

Inserting (12) into (13) and evaluating the derivative therefore yields

$$f(t) = -2\pi h \sum_{n=1}^{N} f_n \left|\beta_n\right| \sin\left(2\pi f_n t + \phi_n\right). \quad (14)$$

Figure 1 illustrates the (normalized) mean power spectrum computed by averaging 10^4 unique CE-OFDM pulsed waveforms comprised of $N = 35$ subcarriers, each modulated with an independent symbol drawn from a 4-QAM constellation, a pulsewidth of $T = 4.5$ μs, and modulation index $h = 0.75$. Inserting these values in (11) yields 36.7 MHz, which fairly closely aligns with the 3-dB bandwidth in Fig. 1.

In comparison, we have also included in Fig. 1 a (normalized) histogram of instantaneous frequency values based on the evaluation of (14) over each of the 10^4 unique CE-OFDM waveforms. Indeed, this result is an even closer fit to a Gaussian shape (as indicated by the dashed trace). The reason for the discrepancy in these two representations is that the mean power spectrum includes the pulse envelope structure, and therefore still exhibits some degree of $sin(x)/x$ spectral roll-off that becomes evident below –30 dB normalized power. In contrast, the instantaneous frequency expression in (14) does not account for the rapid rise/fall at the pulse edges.

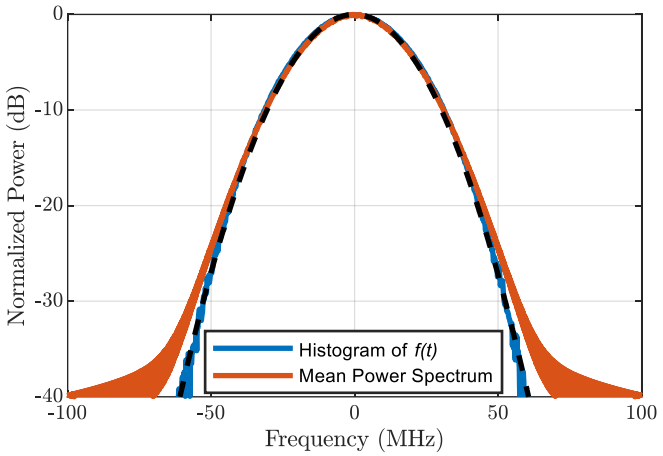

Fig 1. Normalized mean power spectrum and normalized instantaneous frequency histogram for 10^4 unique CE-OFDM waveforms (dashed black trace is the ideal Gaussian shape)

IV. Simulation Analysis

To demonstrate the efficacy of CE-OFDM as a convenient, optimization-free approach to generate RFM radar waveforms, we compare a single waveform instantiation with the coherent combination of 1000 unique CE-OFDM waveforms, where the latter indicates the impact of slow-time processing (i.e. Doppler or cross-range). Here each waveform has a 3-dB bandwidth of 33 MHz and pulsewidth of 4.5 μs, resulting in a per-waveform time-bandwidth product (BT) of 150.

Each unique waveform is comprised of 35 subcarriers that are modulated with symbols independently drawn from a 4-QAM constellation. Figure 2 illustrates the power spectrum obtained from a single random instantiation of a CE-OFDM waveform. It is worth noting that, despite the clear random variation, the expected Gaussian spectrum shape is relatively well maintained even for a single waveform.

The mean power spectrum over the 1000 unique CE-OFDM waveforms does realize a smooth Gaussian shape as illustrated in Fig. 3. A quite similar result is likewise observed in Fig. 3 for two additional sets of 1000 unique CE-OFDM waveforms that are based on 16-QAM and 64-QAM constellations, implying that constellation density provides negligible impact from a radar range sidelobe perspective (since the inverse Fourier transform of a Gaussian spectral density corresponds to a Gaussian autocorrelation).

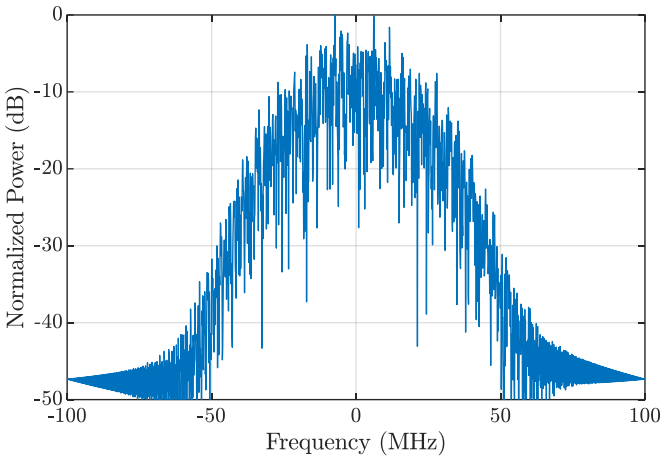

Fig 2. Power spectrum of a single CE-OFDM waveform instantiation

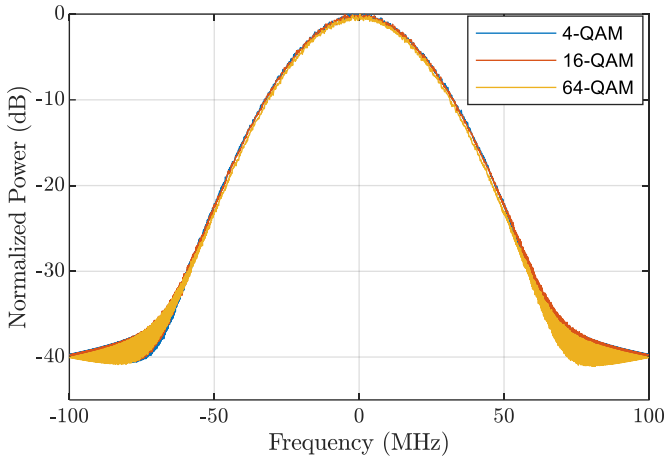

Fig 3. Mean power spectrum over 1000 unique CE-OFDM waveforms

The more interesting comparison (see Fig. 4) is obtained by examining the autocorrelation for the single instantiation of a CE-OFDM waveform relative to the (normalized) coherent combination of autocorrelations of the 1000 unique waveforms (i.e. the zero-Doppler response from slow-time processing). It is observed that, as noted previously for other random FM waveforms [5], the coherent combination of M waveforms provides a sidelobe suppression of $10\log_{10}(M)$ dB due to incoherent sidelobe averaging, while the respective mainlobes remain coherent. Here $10\log_{10}(1000) = 30$ dB of sidelobe suppression is clearly observed.

Figure 5 demonstrates that, as noted in Fig. 3, the constellation size has no noticeable impact on the sidelobe quality of radar performance. Here the coherent combination of autocorrelations for each constellation is compared with the root-mean squared (RMS) autocorrelation response across each set of 1000 unique waveforms, where the latter provides a mean per-waveform performance measure.

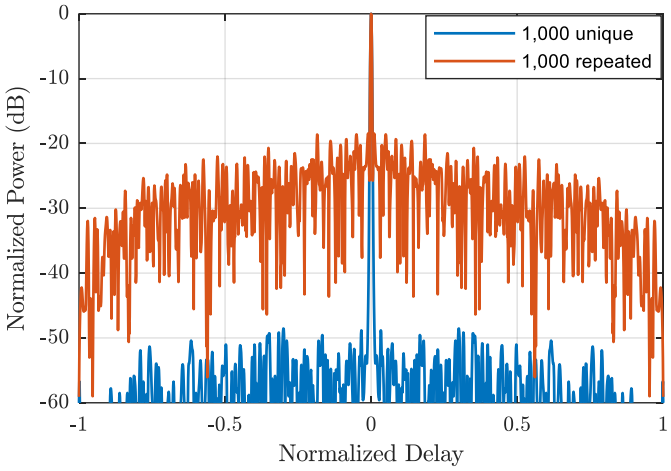

Fig 4. Coherent autocorrelation for 1000 unique CE-OFDM waveforms versus the autocorrelation of a single repeated waveform

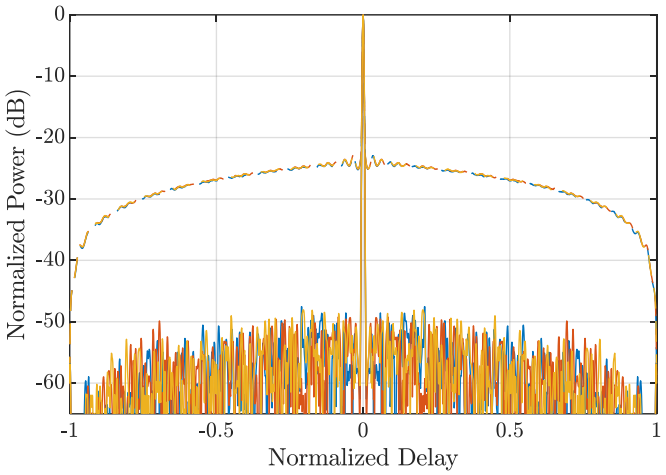

Fig 5. Coherent autocorrelation response (solid) and RMS autocorrelation response (dashed) for 1000 unique CE-OFDM waveforms, for 4-QAM (blue), 16-QAM (orange), and 64-QAM (yellow)

V. Experimental Results

The inherent FM nature of CE-OFDM makes it readily amenable for generation by a high-power radar transmitter with minimal distortion. The importance of this aspect cannot be overstated because CE-OFDM represents a rare intersection of being easily parameterized (for randomized diversity), providing natural spectral shaping of a desirable form (Gaussian), and being readily implementable in radar hardware. In contrast, previous RFM approaches either did not provide spectral shaping [1-4] or necessitated some manner of optimization to achieve it [5-12]. Consequently, we now examine the efficacy of these waveforms experimentally in both loopback and open-air measurement configurations.

A. Loopback Assessment

From a baseband sample rate of 200 MSample/sec each of the 1000 unique waveforms examined in simulation were up-sampled to 12 GSample/sec and then digitally up-converted to a center frequency of 3.55 GHz so they could be implemented on a Tektronix AWG70002A arbitrary waveform generator (AWG), which has a 10-bit depth. Each generated waveform was passed through a class-A amplifier and then an attenuator before being "received", where they were amplified by an LNA to approximate an actual open-loop configuration. The captured signals were recorded using a Rhode & Schwarz FSW real-time spectrum analyzer (RSA).

Figure 6 duplicates the autocorrelation comparison of Fig. 4, albeit now using loopback-captured versions of the waveforms. We again see the same incoherent sidelobe averaging effect that realizes 30 dB suppression for 1000 RFM waveforms. Because no optimization was employed at all here, one can surmise that the benefits of diversity (by way of high dimensionality) may actually outweigh the achievable benefits from trying to optimize any single waveform. Indeed, applying the hyperbolic FM benchmark for peak sidelobe level (PSL) of [33,34]

$$\mathrm{PSL}_{HFM} = [-20\log_{10}(BT) - 3]\ \mathrm{dB} \qquad (15)$$

to a single waveform of $BT = 150$ indicates that the best possible PSL is on the order of -47 dB. Here this value has been surpassed using random (yet structured) waveforms with no optimization whatsoever. The reason for this distinction is the fact that the 1000 unique waveforms with individual $BT = 150$, which per Fig. 5 yield an RMS PSL of about –23 dB, provide an *aggregate time-bandwidth product* of $150\times1000 = 1.5\times10^5$, and it is this greatly expanded dimensionality that is readily compensating for the lack of optimization. Of course, as has been shown previously in [6-11], optimization of individual nonrepeating waveforms can realize even more sidelobe suppression, though at the cost of requiring real-time computation.

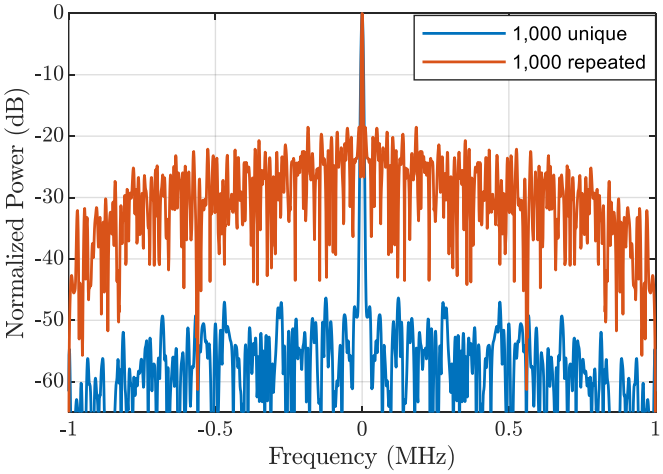

Fig 6. Loopback coherent autocorrelation for 1000 unique CE-OFDM waveforms versus the autocorrelation of a single repeated waveform

B. Open-Air Measurements

An open-air test was performed from the roof of Nichols Hall on the University of Kansas campus using the same waveforms evaluated in loopback. The test setup was directed toward the intersection of 23rd and Iowa Streets to observe moving vehicles. Range-Doppler responses were formed for

three cases: 1) baseline LFM waveform (with same *BT*) repeated over 1000 pulses, 2) a single CE-OFDM waveform repeated over 1000 pulses, and 3) use of the 1000 unique CE-OFDM waveforms. The pulse repetition frequency (PRF) for all three cases was 40 kHz and the three CPIs were repeated nearly back-to-back to try to capture the same moving vehicles. Simple projection-based clutter cancellation was performed since the platform was stationary.

Figure 7 illustrates the baseline case using an LFM waveform. Relatively large movers can be observed, along with the gradual range sidelobe roll-off typical of LFM. While it is true that mismatched filtering via tapering could be employed, we did not do so here to provide a consistent response across the three cases with no SNR loss or resolution degradation incurred.

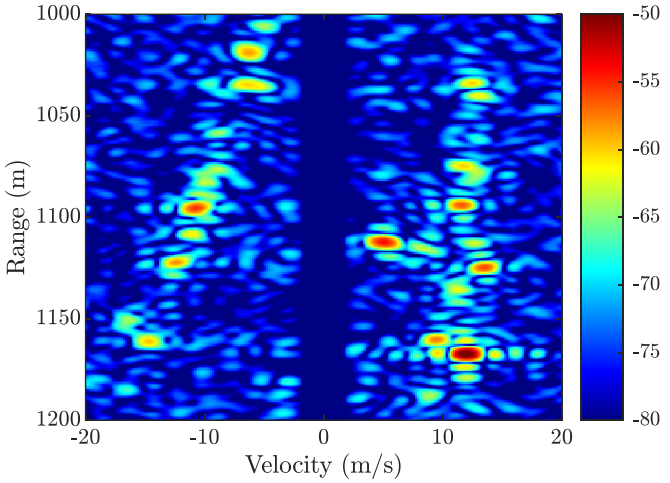

Fig 7. Baseline range-Doppler response (in dBm) for LFM

Figure 8 then depicts the range-Doppler response when a single CE-OFDM waveform is repeated over the 1000-pulse CPI. What is particularly noticeable in this result, relative to the LFM case, is the extended sidelobe floor over most of the range interval in between roughly 9 m/s and 13 m/s in velocity. This phenomenon is a manifestation of the flatter range sidelobe roll-off exhibited by a single waveform in Figs. 4 and 6 (compared to the $sin(x)/x$ sidelobe roll-off of LFM).

In contrast, Fig. 9 shows the range-Doppler response when 1000 unique RFM waveforms based on CE-OFDM are employed. While a precise comparison is difficult since the three CPIs did not illuminate the scene at exactly the same time, one can qualitatively pick out moving targets somewhat more easily.

The main take-away from this result is that CE-OFDM provides a convenient way in which to produce transmitter-amenable RFM radar waveforms that have good per-waveform performance (in terms of range sidelobes) while completely avoiding the need for optimization. The fact that these waveforms are based on a viable communication signal structure, even if CE-OFDM is not as useful as standard OFDM in that regard, means that a DFRC capability is readily available and easy to deploy.

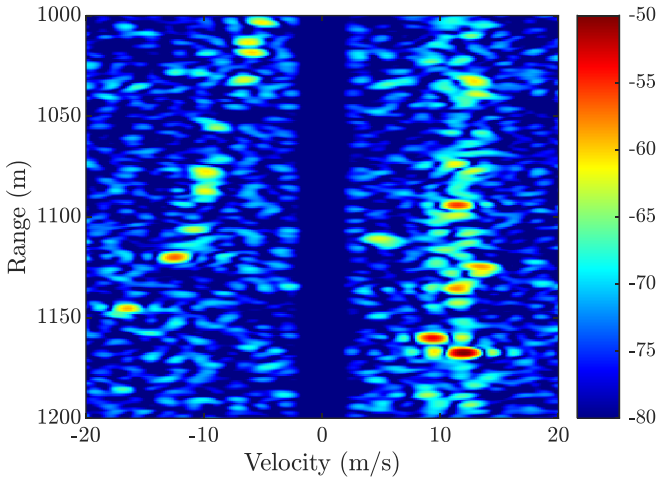

Fig 8. Range-Doppler response (in dBm) for repetition of a single CE-OFDM waveform

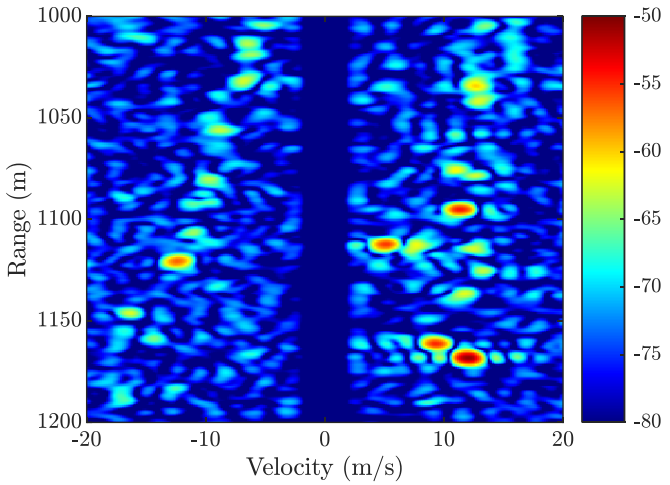

Fig 9. Range-Doppler response (in dBm) for 1,000 unique CE-OFDM waveforms

VI. Conclusions

The CE-OFDM signal structure has previously been proposed as a power-efficient and spectrally-efficient means of communication, though it does involve more complex receive processing than standard OFDM and thus has not been widely used. This signal has also previous been examined as a prospective way in which to design radar waveforms for these same reasons since CE-OFDM essentially represents a form of FM. Here we have extended this premise to evaluate the utility of this waveform class as a convenient approach to construct RFM waveforms that do not repeat over the CPI. Because it avoids the need for per-waveform spectral shaping optimization, while still providing the benefits of RFM, CE-OFDM does indeed enable a readily deployable approach to achieving this capability as well as dual-function radar/communications. Loopback and open-air measurements demonstrate the practical efficacy of this approach from the RFM radar perspective.

REFERENCES

[1] T.B. Whiteley, D.J. Adrian, "Random FM autocorrelation fuze system," U.S. Patent #4,220,952, issued Sept. 2, 1980, application filed Feb. 17, 1956.

[2] L. Guosui, G. Hong, Z. Xiaohua, S. Weimin, "The present and future of random signal radars," *IEEE Aerospace & Electronic Systems Magazine*, vol. 12, no. 10, pp. 35-40, Oct. 1997.

[3] S.R.J. Axelsson, "Noise radar using random phase and frequency modulation," *IEEE Trans. Geoscience & Remote Sensing*, vol. 42, no. 11, pp. 2370-2384, Nov. 2004.

[4] L. Pralon, B. Pompeo, J.M. Fortes, "Stochastic analysis of random frequency modulated waveforms for noise radar systems," *IEEE Trans. Aerospace & Electronic Systems*, vol. 51, no. 2, pp. 1447-1461, Apr. 2015.

[5] S.D. Blunt, et al, "Principles & applications of random FM radar waveform design," to appear in *IEEE Aerospace & Electronic Systems Magazine*.

[6] J. Jakabosky, S.D. Blunt, B. Himed, "Waveform design and receive processing for nonrecurrent nonlinear FMCW radar," *IEEE Intl. Radar Conf.*, Washington, DC, May 2015.

[7] J. Jakabosky, S.D. Blunt, B. Himed, "Spectral-shape optimized FM noise radar for pulse agility," *IEEE Radar Conf.*, Philadelphia, PA, May 2016.

[8] B. Ravenscroft, P.M. McCormick, S.D. Blunt, E. Perrins, J.G. Metcalf, "A power-efficient formulation of tandem-hopped radar & communications," *IEEE Radar Conf.*, Oklahoma City, OK, Apr. 2018.

[9] C.A. Mohr, S.D. Blunt, "FM noise waveforms optimized according to a temporal template error (TTE) metric," *IEEE Radar Conf.*, Boston, MA, Apr. 2019.

[10] C.A. Mohr, P.M. McCormick, S.D. Blunt, C. Mott, "Spectrally-efficient FM noise radar waveforms optimized in the logarithmic domain," *IEEE Radar Conf.*, Oklahoma City, OK, Apr. 2018.

[11] C.A. Mohr, P.M. McCormick, S.D. Blunt, "Optimized complementary waveform subsets within an FM noise radar CPI," *IEEE Radar Conf.*, Oklahoma City, OK, Apr. 2018.

[12] C.A. Mohr, S.D. Blunt, "Design and generation of stochastically defined, pulsed FM noise waveforms," *Intl. Radar Conf.*, Toulon, France, Sept. 2019.

[13] C.-D. Chung, S.-M. Cho, "Constant-envelope orthogonal frequency division multiplexing modulation," *Proc. APCC/OECC*, Beijing, China, Oct. 1999.

[14] S.C. Thompson, A.U. Ahmed, J.G. Proakis, J.R. Zeidler, "Constant envelope OFDM phase modulation: spectral containment, signal space properties and performance," *IEEE Military Communications Conf.*, Monterey, CA, Oct./Nov. 2004.

[15] S.C. Thompson, et al, "Constant envelope OFDM," *IEEE Trans. Communications*, vol. 56, no. 8, pp. 1300-1312, Aug. 2008.

[16] M.P. Wylie-Green, E. Perrins, T. Svensson, "Introduction to CPM-SC-FDMA: a novel multi-access power-efficient transmission scheme," *IEEE Trans. Communications*, vol. 59, no. 7, pp. 1904-1915, July 2011.

[17] J.P. Stralka, "Applications of orthogonal frequency-division multiplexing (OFDM) to radar," PhD dissertation, Johns Hopkins University, Mar. 2008.

[18] S.C. Thompson, J.P. Stralka, "Constant envelope OFDM for power-efficient radar and data communications," *Intl. Waveform Diversity & Design Conf.*, Orlando, FL, Feb. 2009.

[19] S. Sen, A. Nehorai, "Adaptive OFDM radar for target detection in multipath scenarios," *IEEE Trans. Signal Processing*, vol. 59, no. 1, pp. 78-90, Jan. 2011.

[20] S. Liu, Z. Huang, W. Zhang, "A power-efficient radar waveform compatible with communication," *Intl. Conf. Communications, Circuits, & Systems*, Chengdu, China, Nov. 2013.

[21] Q. Zhang, et al, "Waveform design for a dual-function radar-communication system based on CE-OFDM-PM signal," *IET Radar, Sonar & Navigation*, vol. 13, no. 4, pp. 566-572, Apr. 2019.

[22] R. Mohseni, A. Sheikhi, M.A. Masnadi Shirazi, "Constant envelope OFDM signals for radar applications," *IEEE Radar Conf.*, Rome, Italy, May 2008.

[23] S.D. Blunt, M.R. Cook, J. Stiles, "Embedding information into radar emissions via waveform implementation," *Intl. Waveform Diversity & Design Conf.*, Niagara Falls, Canada, Aug. 2010.

[24] C. Sahin, J. Jakabosky, P. McCormick, J. Metcalf, S. Blunt, "A novel approach for embedding communication symbols into physical radar waveforms," *IEEE Radar Conf.*, Seattle, WA, May 2017.

[25] C. Sturm, W. Wiesbeck, "Waveform design and signal processing aspects for fusion of wireless communications and radar sensing," *Proc. IEEE*, vol. 99, no. 7, pp. 1236-1259, July 2011.

[26] A.R. Chiriyath, B. Paul, D.W. Bliss, "Radar-communications convergence: coexistence, cooperation, and co-design," *IEEE Trans. Cognitive Communications & Networking*, vol. 3, no. 1, pp. 1-12, Mar. 2017

[27] S.D. Blunt, E.S. Perrins, eds. *Radar & Communication Spectrum Sharing*, SciTech Publishing, 2018.

[28] L. Zheng, M. Lops, Y.C. Eldar, X. Wang, "Radar and communication coexistence: an overview: a review of recent methods," *IEEE Signal Processing Magazine*, vol. 36, no. 5, pp. 85-99, Sept. 2019.

[29] A. Hassanien, M.G. Amin, E. Aboutanios, B. Himed, "Dual-function radar communications systems: a solution to the spectrum congestion problem," *IEEE Signal Processing Magazine*, vol. 36, no. 5, pp. 115-126, Sept. 2019.

[30] D.A. Hague, P. Kuklinski, "Waveform design using multi-tone feedback frequency modulation," *IEEE Radar Conf.*, Boston, MA, Apr. 2019.

[31] M. Abramowitz, I.A. Stegun, *Handbook of Mathematical Functions with Formulas, Graphs, and Mathematical Tables*, US Dept. of Commerce, 1964, Chap. 9.

[32] B. Ravenscroft, P.M. McCormick, S. Blunt, E.S. Perrins, C. Sahin, J.G. Metcalf, "Experimental assessment of tandem-hopped radar and communications (THoRaCs)," *Intl. Radar Conf.*, Toulon, France, Sept. 2019.

[33] T. Collins, P. Atkins, "Nonlinear frequency modulation chirps for active sonar," *IEE Proc. Radar, Sonar & Navigation*, vol. 146, no. 6, pp. 312-316, Dec. 1999.

[34] S.D. Blunt, E.L. Mokole, "An overview of radar waveform diversity," *IEEE AESS Systems Magazine*, vol. 31, no. 11, pp. 2-42, Nov. 2016.